Comparison of Fourier pseudospectral method seismograms and ray-theory travel times in a simple triclinic model: revealed direct wave

Václav Bucha
Department of Geophysics, Faculty of Mathematics and Physics, Charles University, Ke Karlovu 3, 121 16 Praha 2, Czech Republic, bucha@seis.karlov.mff.cuni.cz

Summary

We calculate a complete seismic wave field using the Fourier pseudospectral method in a simple triclinic velocity model. To identify elementary seismic waves in the complex wave field, we compute ray-theory travel times. The velocity model is composed of two homogeneous layers separated by a curved interface. The anisotropy of the upper layer is triclinic. We show and discuss results of comparison between seismograms and travel times for one common-shot gather.

Keywords

Fourier pseudospectral method, ray-theory travel times, anisotropic velocity model, triclinic anisotropy

1. Introduction

This paper continues testing of the Fourier pseudospectral method started by Bucha (2017b) where he had problems with boundary reflections and identification of one direct wave. The author of the Fourier pseudospectral code, Ekkehart Tessmer, helped to find better absorption parameters at the sides of the model. We used snapshots of the complete wave field and ray-velocity surfaces to reveal the unknown wave as a direct S wave. This wave has not been detected by our ray-theory codes. We present results only for the vertical component of seismic wave field.

The original motivation for the tests was to perform ray-based Kirchhoff prestack depth scalar migration studies in inhomogeneous weakly anisotropic media and test the coupling ray-theory. Ray-theory software package ANRAY and packages MODEL, CRT, FORMS do not offer possibility to calculate coupling ray-theory S waves in models with interfaces. In order to compute synthetic seismograms (recorded wave field), we test the Fourier pseudospectral method (Tessmer, 1995), which enables to calculate synthetic seismograms in 3D heterogeneous anisotropic velocity models with interfaces. We test Fourier pseudospectral method (FM) in a simple triclinic velocity model with one curved interface. To identify elementary waves in the complex wave field, we use ray-based ANRAY software package and compute travel times of twelve elementary waves, both direct and reflected.

The dimensions of the velocity model and shot-receiver configuration for the ray-theory method are the same as in the previous papers by Bucha (e.g., 2012, 2013, 2017a), where we studied the sensitivity of the migrated images to incorrect anisotropy, to incorrect gradients of elastic moduli or to incorrect rotation of the tensor of elastic

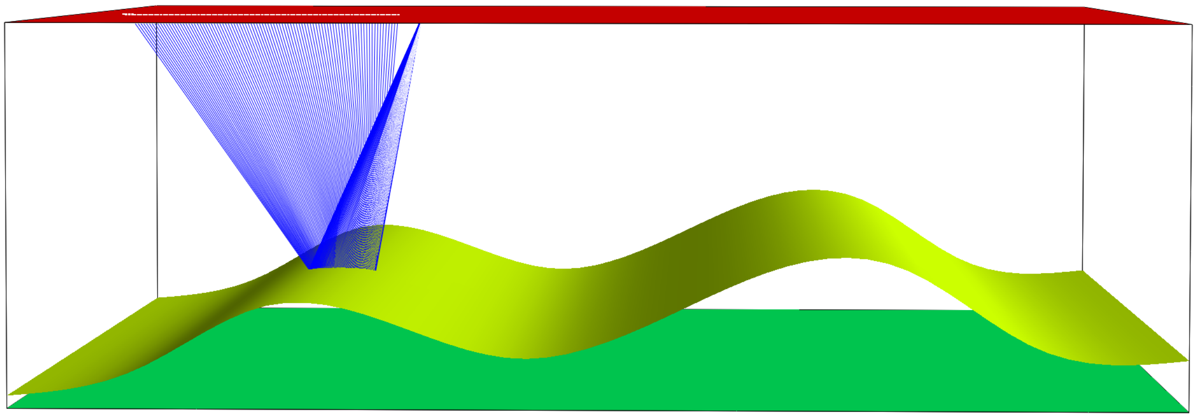

Figure 1. Velocity model with a curved interface. The horizontal dimensions of the velocity model are 0 km $\leq x_1 \leq$ 9.2 km, 0 km $\leq x_2 \leq$ 10 km and the depth is 0 km $\leq x_3 \leq$ 3 km. The velocity model contains one curved interface which is non-inclined in the direction perpendicular to the source-receiver profile. The two-point rays of the converted PS2 wave for one shot-receiver configuration (shot 1) are displayed.

moduli. The simple anisotropic velocity model is composed of two homogeneous layers separated by one curved interface that is non-inclined in the direction perpendicular to the source-receiver profiles. The anisotropy in the upper layer is triclinic and is thus not mirror symmetric. The bottom layer is isotropic. The velocity models for the Fourier method are extended by absorption stripes at the sides.

We display and discuss results of comparison between the Fourier method complete wave field and the ray-theory travel times of twelve elementary waves calculated for one common-shot gather.

2. Triclinic velocity model

The dimensions of the velocity model and measurement configuration are derived from the 2-D Marmousi model and dataset (Versteeg & Grau, 1991). The horizontal dimensions of the velocity model are 0 km $\leq x_1 \leq$ 9.2 km, 0 km $\leq x_2 \leq$ 10 km and the depth is 0 km $\leq x_3 \leq$ 3 km.

Fourier method synthetic seismograms and ray-theory travel times are computed in the velocity model composed of two homogeneous layers separated by one curved interface (see Figure 1). The curved interface is non-inclined in the direction of the x_2 axis which is perpendicular to the source-receiver profile. The medium in the upper layer of this velocity model is triclinic and is represented by the dry Vosges sandstone (Mensch & Rasolofosaon, 1997). The triclinic anisotropy is asymmetric with respect to vertical planes. The matrix of density-reduced elastic moduli in km^2/s^2 reads

$$\begin{pmatrix} 10.3 & 0.9 & 1.3 & 1.4 & 1.1 & 0.8 \\ & 10.6 & 2.1 & 0.2 & -0.2 & -0.6 \\ & & 14.1 & 0. & -0.5 & -1. \\ & & & 5.1 & 0. & 0.2 \\ & & & & 6. & 0. \\ & & & & & 4.9 \end{pmatrix} . \tag{1}$$

The bottom layer in velocity model is isotropic and the P-wave velocity in the bottom layer is $V_p = 3.6$ km/s. The S-wave velocity is $V_s = V_p/\sqrt{3}$.

The S1 and S2 ray-velocity surfaces for triclinic anisotropy have many common, singular points (for figures refer to Bucha, 2017b). Some parts of the surfaces are concave or intersect. All these anomalies cause problems to ray-theory calculation in some directions.

3. Shot and receivers

The measurement configuration is derived from the Marmousi model and dataset (Versteeg & Grau, 1991). For our tests we use the first common-shot configuration only. The profile line is parallel with the x_1 coordinate axis. For ray-theory travel time calculations, the shot is 3 km from the left-hand side of the velocity model (see Figure 1) and the depth of the shot is 0.025 km. The number of receivers per shot is 96. The first receiver is 0.425 km from the left-hand side of the velocity model, the distance between the receivers is 0.025 km, and the depth of the receivers is 0 km. To calculate the Fourier method seismograms, we use models enlarged by absorbing stripes at the sides, hence the common-shot configuration has to be shifted with respect to the new sides and starts at different coordinates.

4. Fourier pseudospectral method

To calculate the complete wave field for one common-shot gather, we apply code FT43DANX by E. Tessmer (Tessmer, 1995). The code is based on the Fourier method (FM), a kind of pseudospectral method (e.g., Kosloff & Baysal, 1982). The code FT43DANX was previously used to test the accuracy of coupling ray theory and standard ray theory results in 3D inhomogeneous, weakly anisotropic media without interfaces (Pšenčík, Farra & Tessmer, 2011; Bulant et al., 2011). This implementation of the FM is applicable to any type and strength of anisotropy. It works equally well in regular as well as in singular regions of the ray method.

In the Fourier method, spatial first derivatives in the elastodynamic equation are calculated with very high accuracy in the wavenumber domain using fast Fourier transforms (FFT) as follows: (a) forward FFT of the wave field along the desired direction, (b) multiplication of the components of the wavenumber spectrum with the respective wave numbers times the imaginary unit, and (c) inverse FFT of the result of (b). Computations with the Nyquist wave numbers are avoided by using odd-numbered FFT lengths. For more information about the Fourier method refer to Tessmer (1995) and Pšenčík, Farra & Tessmer (2011).

The algorithm is based on a regular numerical grid. For simple structures with horizontal layering, the input parameters for velocity model are located in the main ASCII input file. The velocity model for our tests contains a curved interface. In such a case, the input structure for code FT43DANX needs to be gridded and saved in a separate binary file. We performed gridding of the velocity model using MODEL and FORMS packages (Červený, Klimeš & Pšenčík, 1988; Bucha & Bulant, 2017). There are two limitations for setting grid sizes. The first is that the grid size numbers must be factorizable into the factors up to 23, and the FFT algorithm is the more efficient the smaller factors are. The second limitation is connected with the first one, the grid sizes must be odd numbers.

To avoid wrap-around or boundary reflections, the model is surrounded by sponge-like absorbing regions (Cerjan et al., 1985). This requires the numerical grid to be extended at its sides. We present calculations with 50 grid points at the sides of the model which seem to be slightly better than for 20 grid points.

We use an explosive source for calculation of ray-theory synthetic seismograms. The source-time function is a Gabor wavelet, $\exp[-(2\pi f/\gamma)^2 2t^2]\cos(2\pi ft)$, with the dominant frequency $f = 25$ Hz and $\gamma = 4$. The time step for wave field calculation is 0.004 s and the propagation time starts at 0 s and ends at 2.5 s. The source must be away from the surface. Sources and receivers should be at least 5 grid points away from the absorbing boundaries. Source and receiver positions are specified by grid indices.

Due to the above mentioned limitations and requirements, it is not easy to find the suitable computational grid parameters. Moreover, numerical algorithms based on pseudospectral methods are computationally more expensive than finite-difference methods. We tested the Fourier method with various values of input parameters. The results in the paper correspond to our best selection up to date.

5. Ray-theory travel times

Ray-theory travel times in the triclinic velocity model are computed using the ANRAY software package (Gajewski & Pšenčík, 1990). 3-D ray tracing is used to calculate the two-point rays of 12 elementary waves: direct P, S1, S2 waves, reflected P, S waves and converted waves. The source is an explosion and the source wavelet is the Gabor function with the prevailing frequency of 25 Hz, and the time step is 0.004 s. The same wavelet as in the Fourier method calculations is applied. For comparison with FM seismograms, we use the plots of travel times because they are more illustrative than the plots of seismograms of individual elementary waves.

6. Comparison of seismic wave field and travel times

The Fourier method calculates many waves in regions where the ray-theory method fails. For plotting of Fourier method (FM) seismograms, we use the Seismic Unix plotting tools (Cohen & Stockwell, 2013). We display ANRAY travel times together with converted FM seismograms using MODEL and FORMS packages. We use different amplitude scaling for converted FM seismograms to make the figures with travel times clearer. Seismograms and travel times are plotted up to the time 2.5 s. In the paper, we show the FM results for enlarged model with 50 absorption grid points at the sides of the velocity model.

The velocity model with 50 absorption grid points at the sides of the model use numerical grid $495 \times 225 \times 243$ grid nodes in x_1, x_2 and x_3 directions, respectively. The grid steps are 0.025 km. The horizontal dimensions of the velocity model are 0 km $\leq x_1 \leq$ 12.35 km, 0 km $\leq x_2 \leq$ 5.6 km and the depth is 0 km $\leq x_3 \leq$ 6.05 km. The shot is 4.2 km from the left-hand side of the enlarged velocity model and the depth of the shot is 2.025 km. The number of receivers per shot is 96. The first receiver is 1.625 km from the left-hand side of the velocity model, the distance between the receivers is 0.025 km, and the depth of the receivers is 2 km.

The author of the Fourier pseudospectral code, Ekkehart Tessmer, recommended us better absorption parameters at the sides of the model. The improvement is obvious when we compare Figure 3 with Figure 4. A relatively strong wave starting at 1.8 s (at the left hand side) in Figure 3 is not detected in Figure 4. Figure 3 was calculated with old absorption parameters (Bucha, 2017b). We suppose that this wave most probably belongs to the reflection from the free surface.

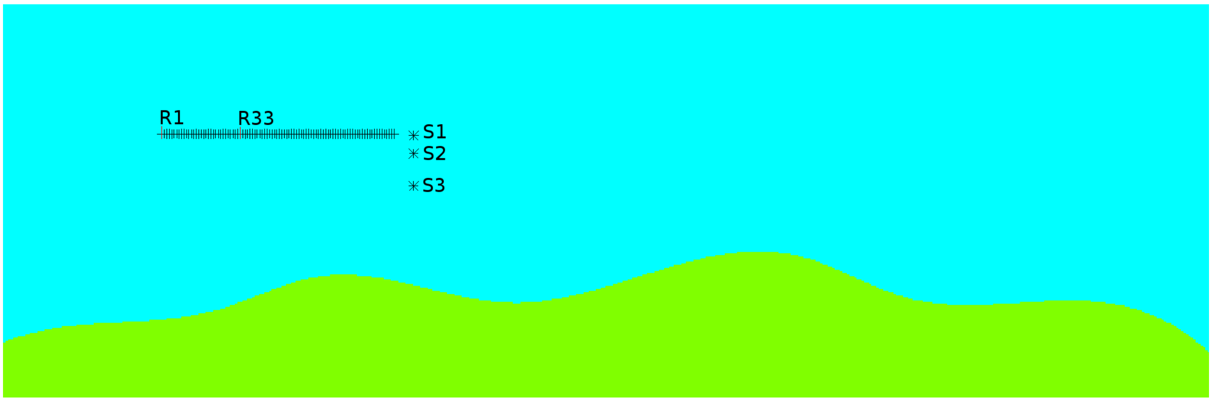

Figure 2. Section of the enlarged velocity model with 50 absorption grid points for the FM calculation. The dimensions of the section are 0 km $\leq x_1 \leq$ 12.35 km and 0 km $\leq x_3 \leq$ 6.05 km. The velocity model contains one curved interface which is non-inclined in the direction perpendicular to the source-receiver profiles. Shot S1 is at the depth=2.025 km, shot S2 is at the depth=2.275 km and shot S3 is at the depth=2.775 km. The first receiver is 1.625 km from the left-hand side of the velocity model, and the depth of the receivers is 2 km.

It is not easy to recognize elementary waves in the complete wave field calculated by the Fourier method. Figure 5 with ray-theory travel times of 12 elementary waves should help to identify some parts of FM seismograms. Direct P, S1 and S2 waves are denoted by coloured octagon symbols. Reflected P, S1, S2 and converted waves are denoted by coloured asterisk symbols. Some of travel time curves or parts of them fit arrivals in FM seismograms. Some of them are questionable.

To see the details of the FM seismogram and the ray-theory travel times, we display in Figure 6 one trace at receiver 33 (from the left-hand side of Figures 4 and 5). The detailed view shows some other wave in the part between the direct P and S2 wave. The amplitude of this wave is the strongest in the seismogram. The unknown wave is better visible in Figure 7 where we plot one trace at receiver 1 and we shortened the plotted time interval.

To reveal the wave between the direct P and S2 wave we firstly calculated seismograms for two other different depths of the source (see Figure 2). The position of receivers is for all tests the same. Seismogram in Figure 7 corresponds to the source S1 (original position) at the depth=2.025 km. Figure 8 shows seismogram for source S2 at the depth=2.275 km. Note that the amplitude of the unknown wave is relatively smaller than in Figure 7. Seismogram for the last tested source S3 at the depth=2.775 km is displayed in Figure 9. Here the unknown wave is not present. Figure 10 shows seismograms for source S3 and all 96 receivers (compare with Figure 4). Tests with different depths of the source revealed that the existence of unknown wave is directionally dependent.

In the next step of our tests, we calculated and plotted snapshots of the wave field (Figure 11). It is obvious that the unknown direct wave between P and S2 wave is also S2 wave caused by triplication. For comparison we plotted ray-velocity surfaces. Figure 12 displays the sliced P, S2 and S1 wave ray-velocity surfaces for the triclinic anisotropy. The triplication of S2 wave is visible. The reason why we did not detected revealed S2 wave by the ray-theory code will be subject of further study.

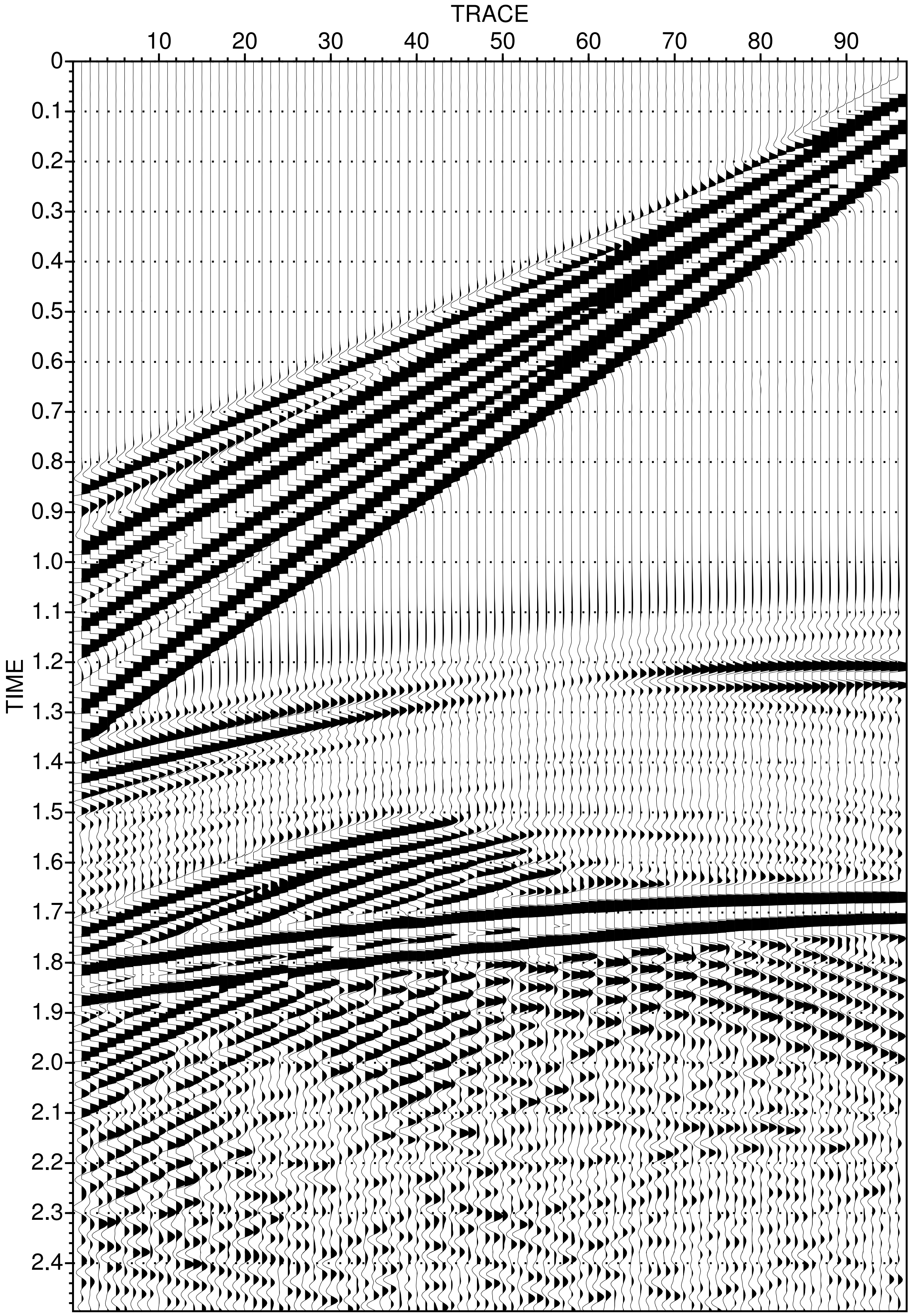

Figure 3. Seismograms calculated using the FM method, with old absorption parameters, for one common-shot gather.

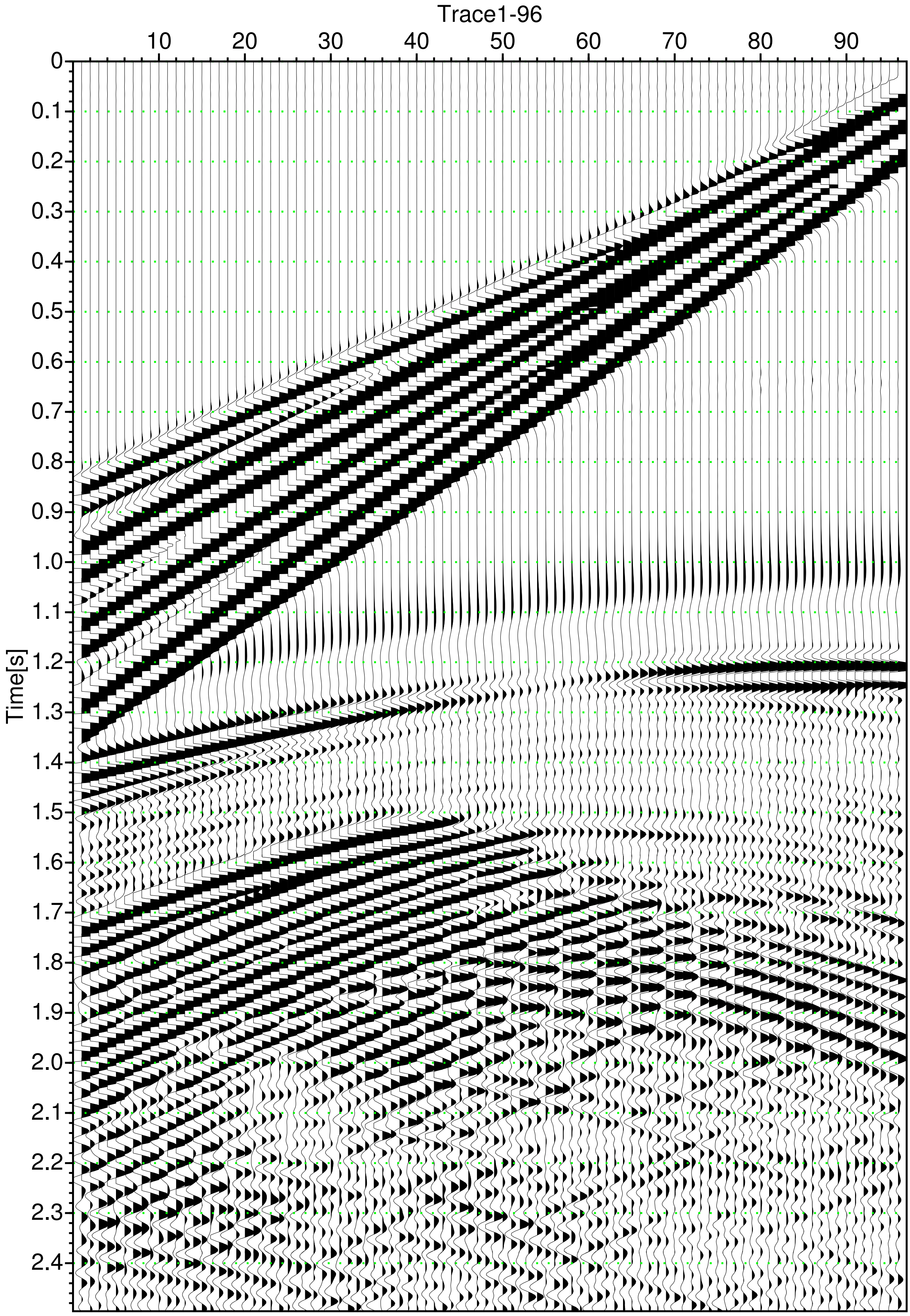

Figure 4. Seismograms calculated using the FM method for one common-shot gather. Amplitudes are filled and magnified more than in Figure 5.

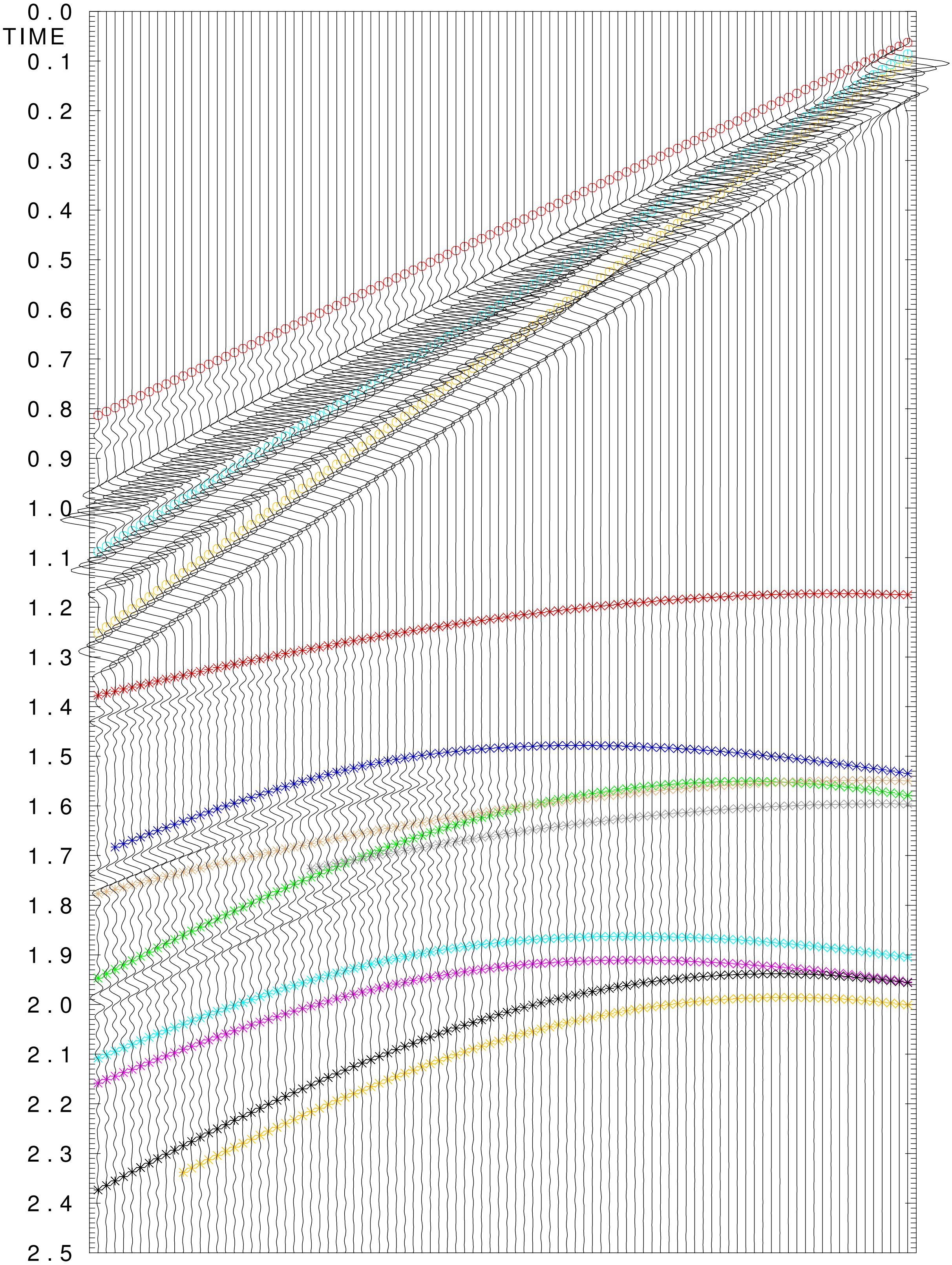

Figure 5. Seismograms calculated using the FM method and travel times calculated using the ANRAY package for one common-shot gather. Plotted travel times correspond to the direct P, S1, S2, reflected P, S and converted waves. The 12 elementary waves, ordered approximately according to travel time from the smallest, are direct (octagon symbol) **P** wave, **S2** wave, **S1** wave, reflected (asterisk symbol) **PP** wave, **PS2** wave, **PS1** wave, **S2P** wave, **S1P** wave, **S2S2** wave, **S1S2** wave, **S2S1** wave and **S1S1** wave.

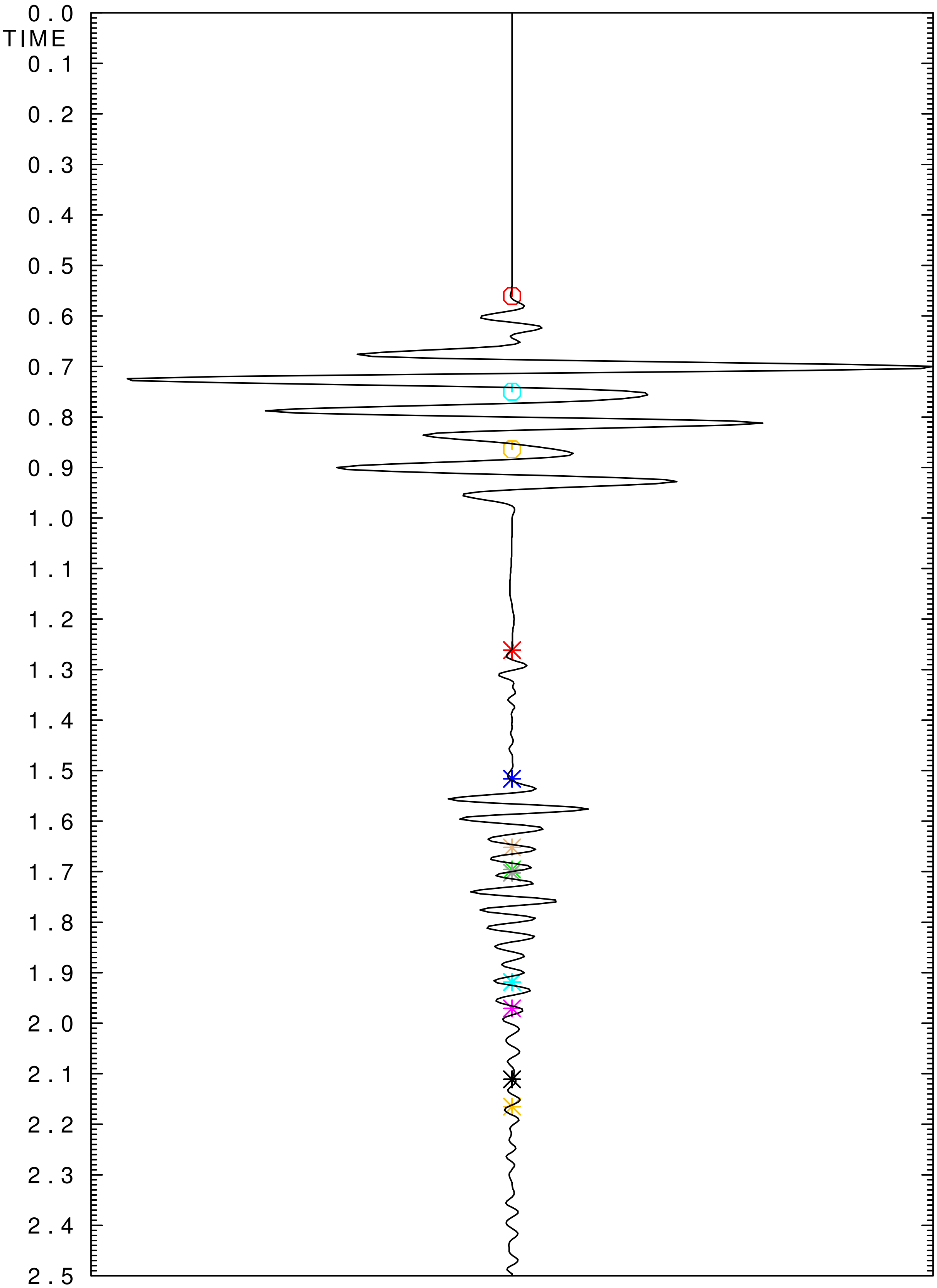

Figure 6. Seismogram calculated using the FM method and travel times calculated using the ANRAY package for receiver 33 (from the left-hand side of Figures 4 and 5). Plotted travel times correspond to the direct P, S1, S2, reflected P, S and converted waves. The 12 elementary waves, ordered approximately according to travel time from the smallest, are the direct (octagon symbol) **P** wave, **S2** wave, **S1** wave, the reflected (asterisk symbol) **PP** wave, **PS2** wave, **PS1** wave, **S2P** wave, **S1P** wave, **S2S2** wave, **S1S2** wave, **S2S1** wave and **S1S1** wave.

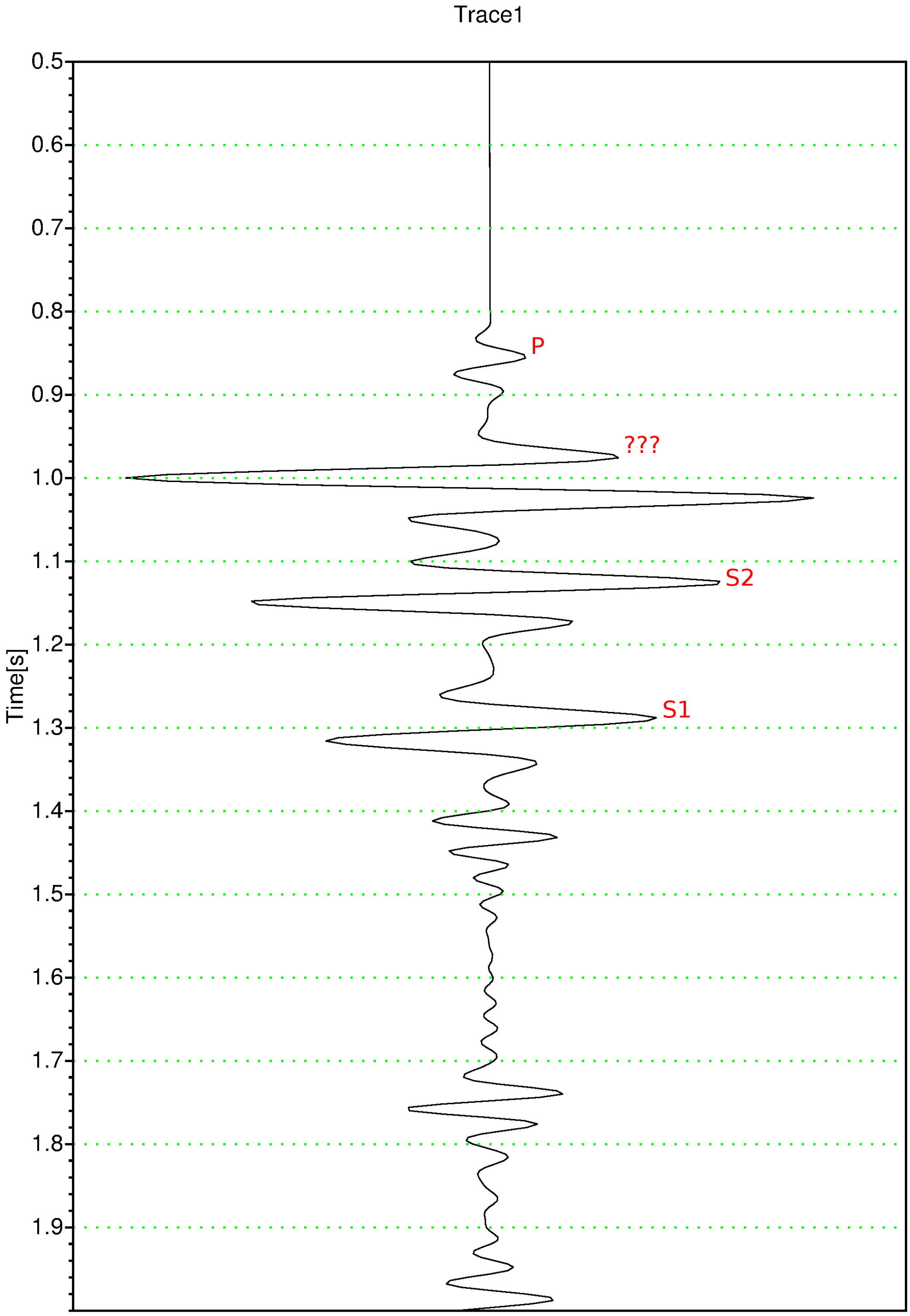

Figure 7. Seismogram calculated using the FM method for receiver 1 (from the left-hand side of Figures 4 and 5). We use source **S1** at the **depth=2.025 km**, receivers are at the depth=2.000 km.

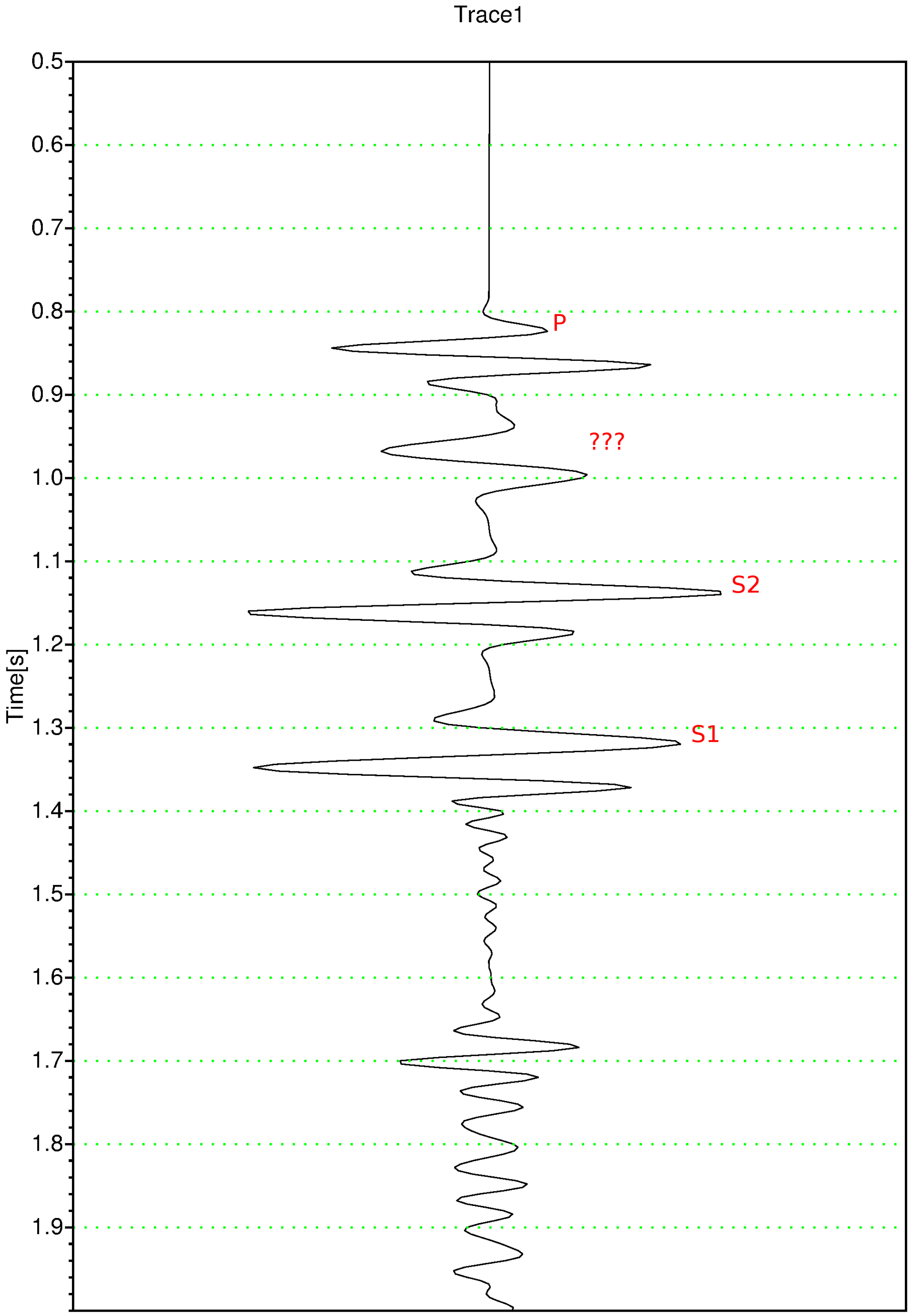

Figure 8. Seismogram calculated using the FM method for receiver 1 (from the left-hand side of Figures 4 and 5). We use source **S2** at the **depth=2.275 km**, receivers are at the depth=2.000 km.

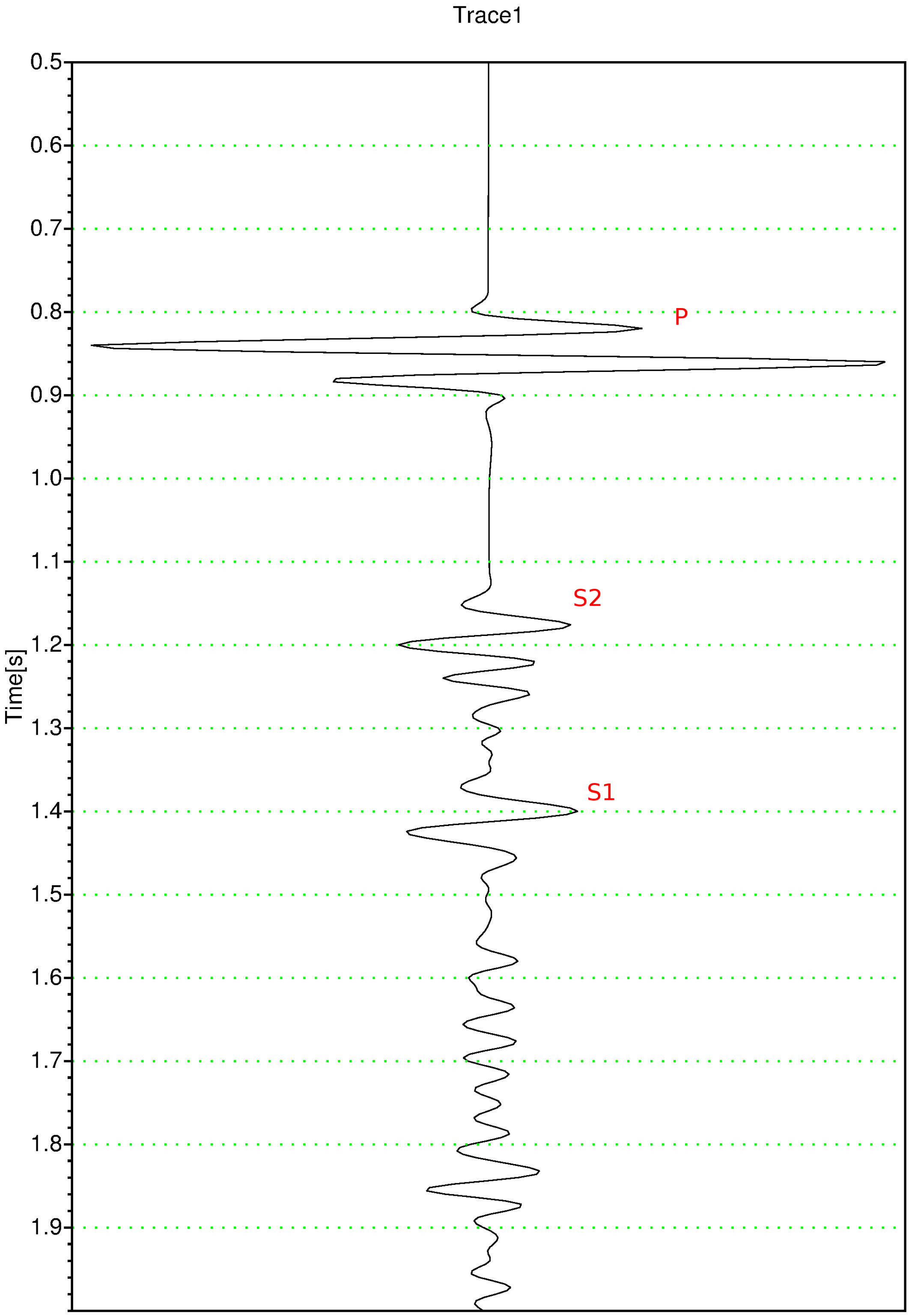

Figure 9. Seismogram calculated using the FM method for receiver 1 (from the left-hand side of Figures 4 and 5). We use source **S3** at the **depth=2.775 km**, receivers are at the depth=2.000 km.

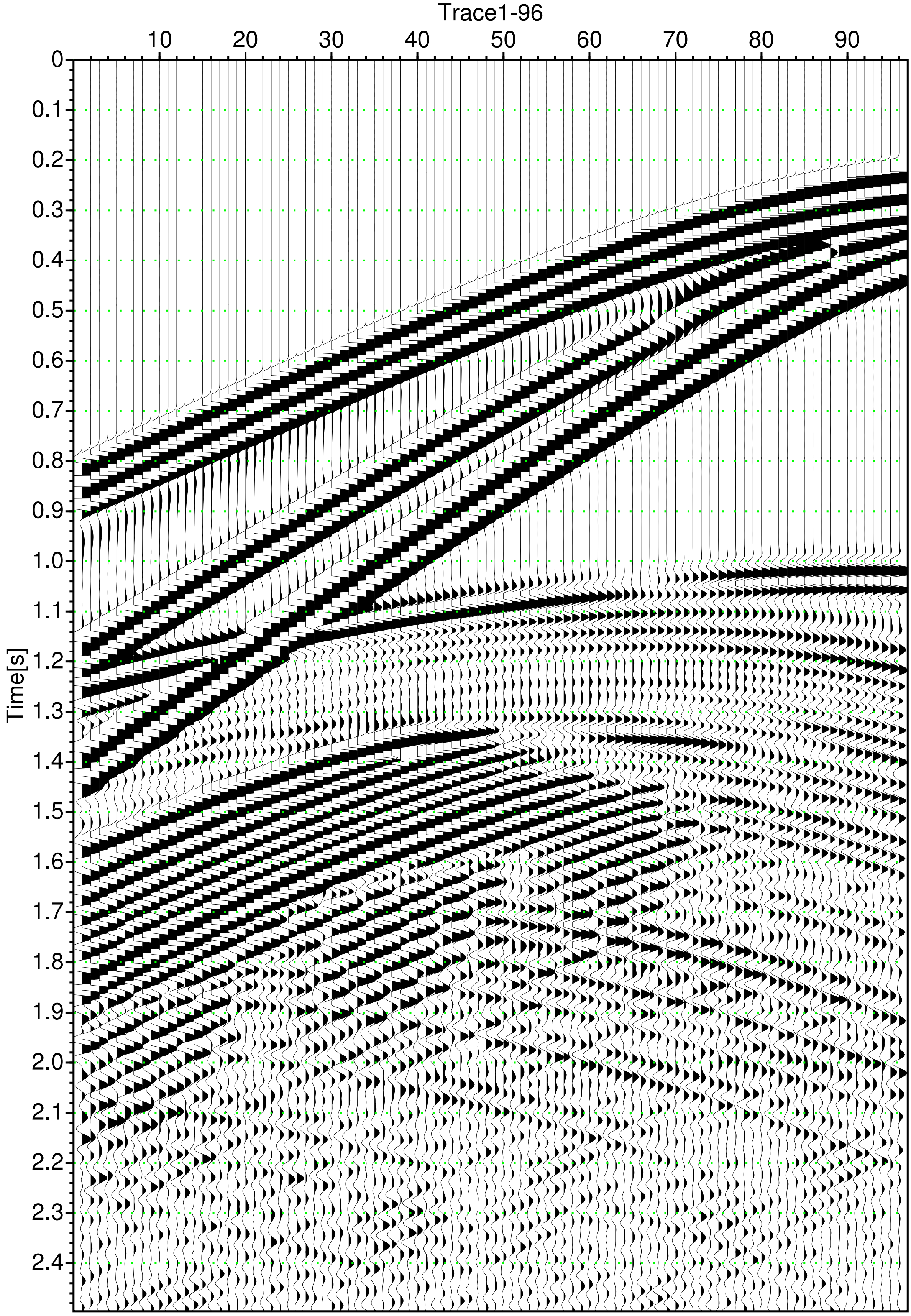

Figure 10. Seismograms calculated using the FM method for 96 receivers. We use source **S3** at the **depth=2.775 km**, receivers are at the depth=2.000 km.

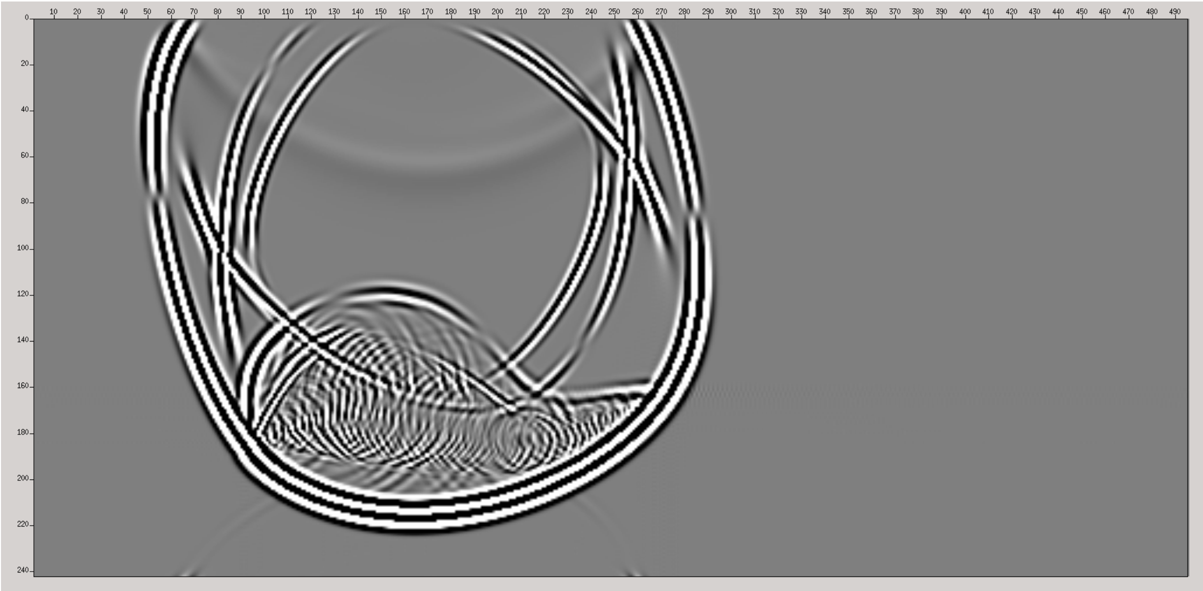

Figure 11. Snapshot of the wave field for one common-shot gather.

7. Conclusions

We have presented improved results of comparison between the Fourier method synthetic seismograms and the ray-theory travel times for one common shot gather. New absorption parameters at the sides of the model suppressed better boundary reflections. Snapshots of the complete wave field and ray-velocity surfaces helped us to reveal the unknown wave as direct S2 wave. This wave was not detected by the ray-theory code. We have presented results only for vertical component of seismic wave field.

Acknowledgements

The author thanks Ekkehart Tessmer for his help and providing the Fourier method code. The author also thanks to Ivan Pšenčík and Luděk Klimeš for their help throughout the work on this paper.

The research has been supported by the Grant Agency of the Czech Republic under Contract 16-05237S, by the Ministry of Education of the Czech Republic within Research Project CzechGeo/EPOS LM2015079, and by the members of the consortium "Seismic Waves in Complex 3-D Structures" (see "http://sw3d.cz").

References

Bucha, V. (2012): Kirchhoff prestack depth migration in 3-D simple models: comparison of triclinic anisotropy with simpler anisotropies. *Stud. geophys. geod.*, **56**, 533–552.

Bucha, V. (2013): Kirchhoff prestack depth migration in velocity models with and without vertical gradients: Comparison of triclinic anisotropy with simpler anisotropies. In: *Seismic Waves in Complex 3-D Structures*, **23**, 45–59, online at "http://sw3d.cz".

Bucha, V. (2017a): Kirchhoff prestack depth migration in simple models with differently rotated elasticity tensor: orthorhombic and triclinic anisotropy. *J. seism. Explor.*, **26**, 1–24.

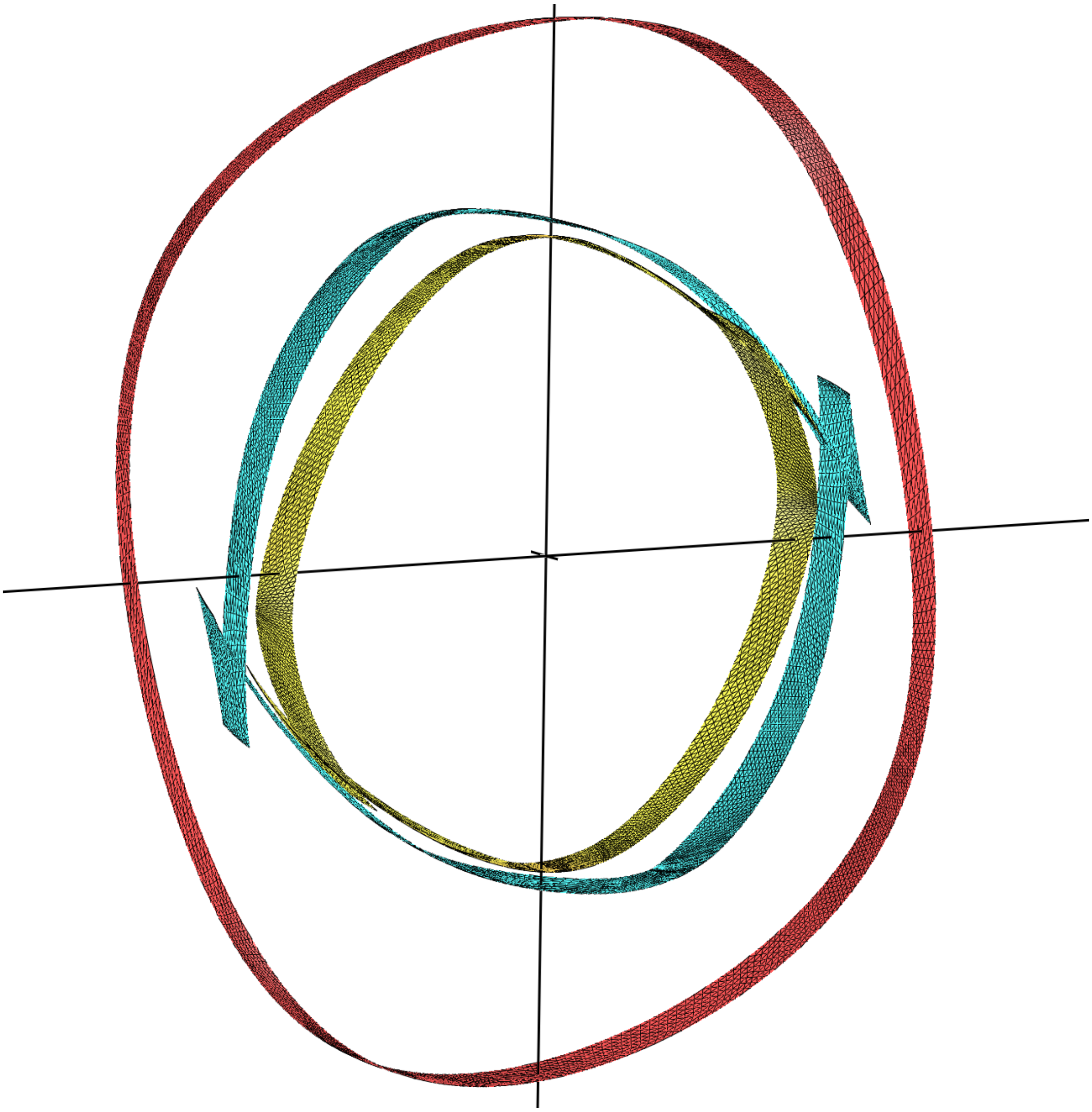

Figure 12. The sliced P, S2 and S1 wave ray-velocity surfaces for the triclinic anisotropy.

Bucha, V. (2017b): Comparison of Fourier pseudospectral method seismograms and ray-theory travel times in a simple triclinic model. *Seismic Waves in Complex 3-D Structures*, **27**, 69–82, online at "http://sw3d.cz".

Bucha, V. & Bulant, P. (eds.) (2017): SW3D-CD-21 (DVD-ROM). *Seismic Waves in Complex 3-D Structures*, **27**, 133–134, online at "http://sw3d.cz".

Bulant, P., Pšenčík, I., Farra, V. & Tessmer, E. (2011): Comparison of the anisotropic-common-ray approximation of the coupling ray theory for S waves with the Fourier pseudo-spectral method in weakly anisotropic models. In: *Seismic Waves in Complex 3-D Structures*, **21**, 167–183, online at "http://sw3d.cz".

Cerjan, C., Kosloff, D., Kosloff, R. and Reshef, M. (1985): A non-reflecting boundary condition for discrete acoustic and elastic wave calculation. *Geophysics*, **50**, 705–708.

Červený, V., Klimeš, L. & Pšenčík, I. (1988): Complete seismic-ray tracing in three-dimensional structures. In: Doornbos, D.J. (ed.), *Seismological Algorithms*, Academic Press, New York, pp. 89–168.

Cohen, J. K. & Stockwell, Jr. J. W. (2013): CWP/SU: Seismic Un*x Release No. 43R5: an open source software package for seismic research and processing, Center for Wave Phenomena, Colorado School of Mines.

Gajewski, D. & Pšenčík, I. (1990): Vertical seismic profile synthetics by dynamic ray tracing in laterally varying layered anisotropic structures. *J. geophys. Res.*, **95B**, 11301–11315.

Kosloff, D. & Baysal, E. (1982): Forward modeling by a Fourier method. *Geophysics*, **47**, 1402–1412.

Mensch, T. & Rasolofosaon, P. (1997): Elastic-wave velocities in anisotropic media of arbitrary symmetry-generalization of Thomsen's parameters ϵ, δ and γ. *Geophys. J. Int.*, **128**, 43–64.

Pšenčík, I., Farra, V. & Tessmer, E. (2011): Comparison of the FORT approximation of the coupling ray theory with the Fourier pseudospectral method. In: *Seismic Waves in Complex 3-D Structures*, **21**, 129–166, online at "http://sw3d.cz".

Tessmer, E. (1995): 3-D seismic modeling of general material anisotopy in the presence of the free surface by a Chebychev spectral method. *Geophys. J. Int.*, **121**, 557–575.

Versteeg, R. J. & Grau, G. (eds.) (1991): The Marmousi experience. *Proc. EAGE workshop on Practical Aspects of Seismic Data Inversion (Copenhagen, 1990)*, Eur. Assoc. Explor. Geophysicists, Zeist.